Supplementary information

Generic acquisition protocol for quantitative MRI of the spinal cord

In the format provided by the authors and unedited

Supplementary material

Alternative techniques not included in the protocol

In this section we discuss alternative techniques to those included in the proposed protocol. These may include techniques that are still at the research stage but could eventually be added to the protocol.

Advanced Shimming

The default shim coils that are integrated in the MR system are usually not sufficient for compensating for the high spatial variations of the magnetic field across the SC axis, which has motivated the development of custom high-order shim coils [1,2].

Another approach to further minimize B_0 inhomogeneities is dynamic shimming, wherein shim coefficients are set for each slice independently. This approach only works for 2D imaging, but is particularly useful for axial EPI acquisitions. In the case of fieldSC imaging where axial slices are relatively thick (3-5mm), the dominant effect of field inhomogeneity is along the z direction (superior-inferior axis). Researchers have thus proposed to only correct for induced gradient fields along this axis, naming the approach z-shimming [3,4]. This technique has shown substantial improvement in image quality for gradient-echo EPI, notably by reducing signal dropout, which is typically observed at the vicinity of intervertebral discs. For more details on shimming strategies for SC imaging, see [5].

Another important effect to consider is the dynamic nature of the B_0 field, as it varies throughout respiration. This effect is particularly problematic when imaging close to the lungs, e.g. around vertebral levels C7-T1. B_0 variation can be up to 70 Hz at 3T [6] and 110 Hz at 7T [7], causing voxel displacement in EPI readout and ghosting in EPI and non-EPI imaging. To tackle this issue, real-time shimming can be used, which consists in varying the shimming gradients during the subject's breathing, as was demonstrated in the brain at 7T [8] and for the spinal cord at 3T [2]. All these advanced techniques are being actively developed, so there is hope that vendors will rapidly translate some of these innovations into widely-available products.

Navigator echoes

Navigator echoes can be used to measure drift in the B_0 field, which can then be used to adjust the excitation frequency and/or the filling of k-space. This technique notably helps reduce ghosting and is important to ensure proper reconstruction of readout-segmented EPI sequences [9]. Navigators are effective for brain scans where most of the region of interest occupies the acquired volume. However, when applied to the SC area, they can create spurious phase offsets. This is because the SC represents a small portion of the acquired volume, shows a relatively poor shim, and is prone to multiple non-linear motions (e.g. muscles move

independently of the cord), leading to complex spatio-temporal phase distributions. One approach that seems promising is that of 2D or 3D navigators [10], whereby only a portion of the volume is selected to estimate phase dynamics. 2D or 3D navigator echoes could potentially be incorporated into the DWI sequence that is part of the *spine generic* protocol.

B1+ mapping

RF transmit field (B1+) maps are used in qMRI to correct for B1+ inhomogeneity-induced signal intensity variation. This can be particularly useful for obtaining accurate T1 [11] and MT measurements [12] and has recently been incorporated within the MTsat protocol [13]. B1+ maps can also be used for shimming the RF field in parallel transmit systems [14], which is of particular interest at ultra-high field strengths where dielectric artifacts present significant challenges for qMRI. B1+ maps can be obtained using a standard product double angle EPI sequence [12]. Some other commonly used methods include magnetization prepared TurboFLASH [15], spin-echo/stimulated-echo acquisition [16], actual flip angle imaging [17], the DREAM sequence [18] and the Bloch Siegert method [19]. B1+ mapping is not currently included in the *spine generic* protocol but the protocol could be extended to do so.

Phase sensitive inversion recovery (PSIR)

In the last decade, sagittal turbo spin echo phase sensitive inversion recovery (PSIR) protocols have been successfully applied to SC imaging of MS patients and those with radiologically isolated syndrome (RIS) for lesion detection [20–22]. In 2013, an axial 3D gradient echo PSIR protocol was successfully applied for the first time in the SC of MS patients using a Philips scanner, showing very good gray matter/white matter/lesion contrast [23,24]. A clinically feasible gradient echo 2D PSIR protocol (about 2 minutes to acquire a single slice) was developed in 2015 on a Siemens 3T scanner [25]. That 2D PSIR protocol has been assessed between the three major MRI vendors [26] and used to measure *in vivo* GM and WM areas at multiple SC levels (cervical and thoracic) in MS patients [27,28], motor neuron disease patients [29] and healthy controls [30,31].

Reconstruction, interpolation, filters

Interpolation (e.g., via zero filling) is not recommended because it (i) can be done during post-processing, (ii) takes more physical space for MRI raw data, and (iii) can introduce confusion as to what is the native resolution when sharing NIfTI data or publishing results. Related to this point, it is important to bear in mind that the true, Fourier resolution may be in general lower than the image spatial resolution (i.e. the nominal, physical pixel spacing), owing to point spread function blurring in k-space. This effect may be stronger for sequences featuring long echo trains, as for example fast spin echo (for T2w anatomical imaging) or EPI (for diffusion).

Procedure

Subject preparation

Positioning and immobilization strategies

A cervical collar is effective for reducing motion [32]. However, some disadvantages include that it may: (i) not fit in the coil (e.g., 64ch), (ii) increase the natural cervical cord lordosis, (iii) create discomfort for some subjects.

Custom tight-fitting helmets, such as the CaseForge (https://caseforge.co/), are personalized helmets that fit perfectly in specific coil models. Their use has been shown to lead to highly reproducible positioning throughout longitudinal studies [33], however, they require customization and, hence, are not a viable solution for large-scale multi-center studies.
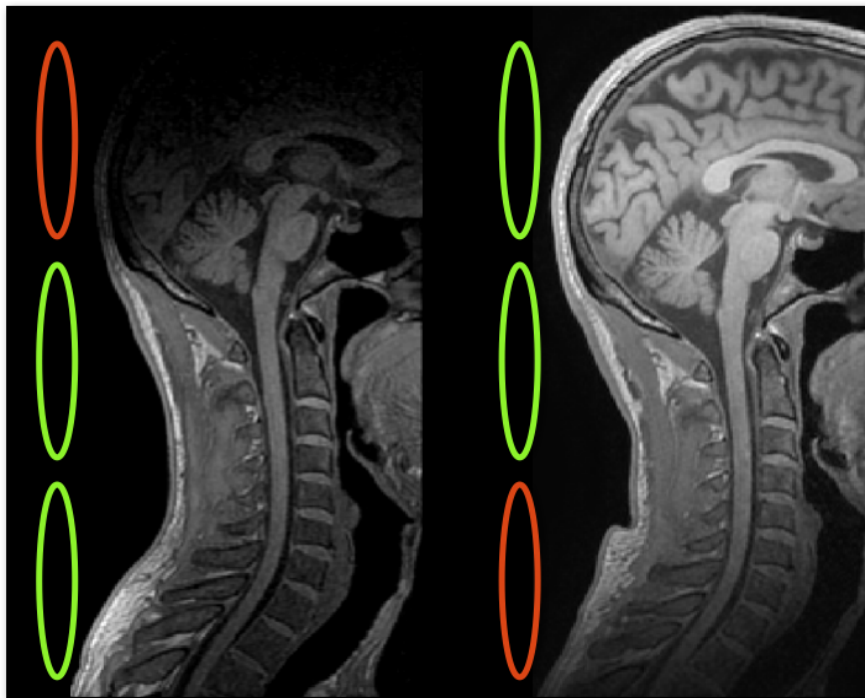
Troubleshooting

Figure S1. *Illustration of the effect of not using the appropriate coil and/or not selecting the appropriate elements. On the left, the head coil elements (shown in red) were inactive during acquisition of the T1w scan (step 6), resulting in insufficient signal in the head region. On the right, the elements corresponding to the lower c-spine were inactive, resulting in low signal in this region.*
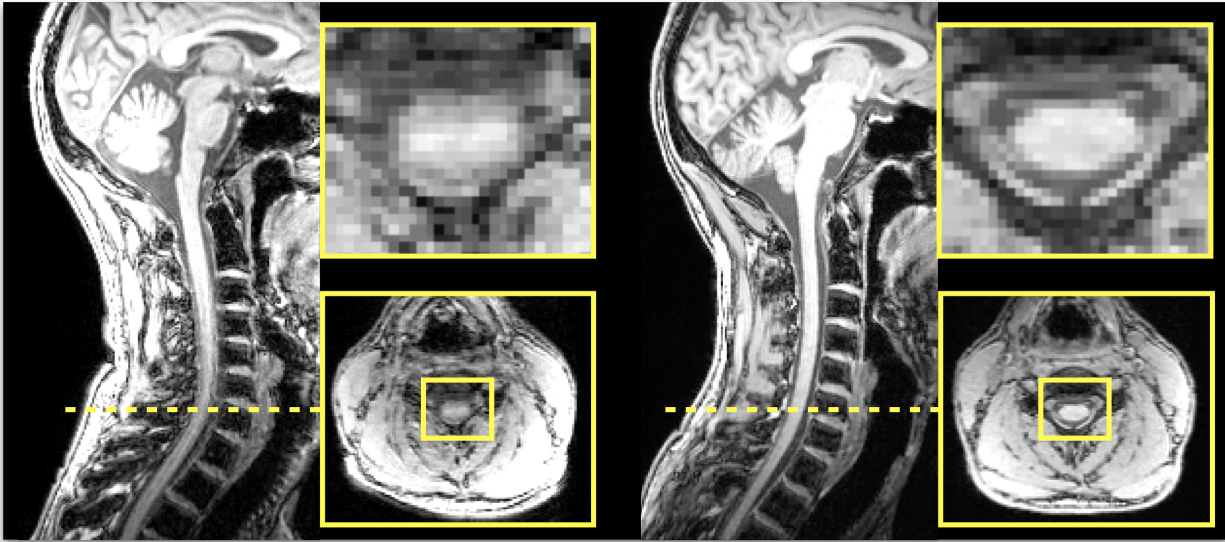
Figure S2. *T1w MPRAGE taken in the same subject (from the single-subject database) at two different sites on a Siemens Prisma system. The slightly larger cervical lordosis on the left likely induced more pronounced CSF flow and SC motion resulting in the artifact shown in the axial view.*
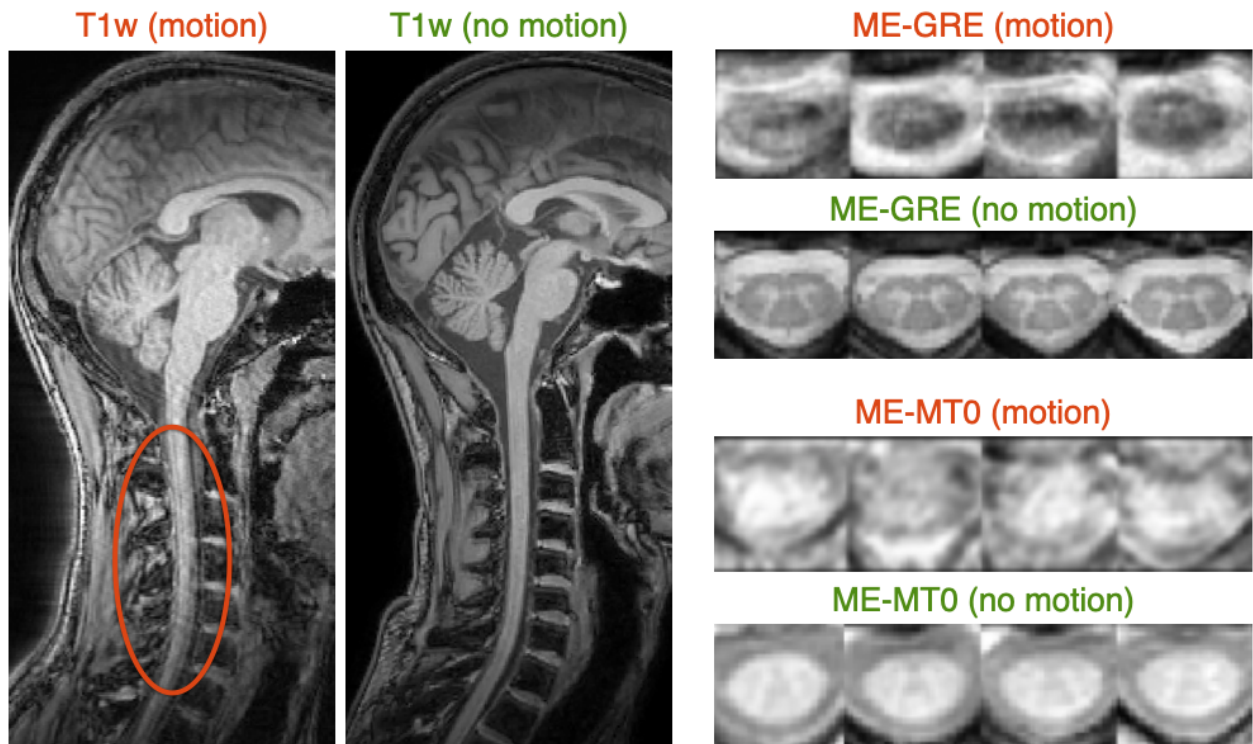

Figure S3. *Illustration of the effect of subject motion on T1w (step 6), ME-GRE (step 8) (zoomed view) and ME-MT0 scans (step 9) (zoomed view).*
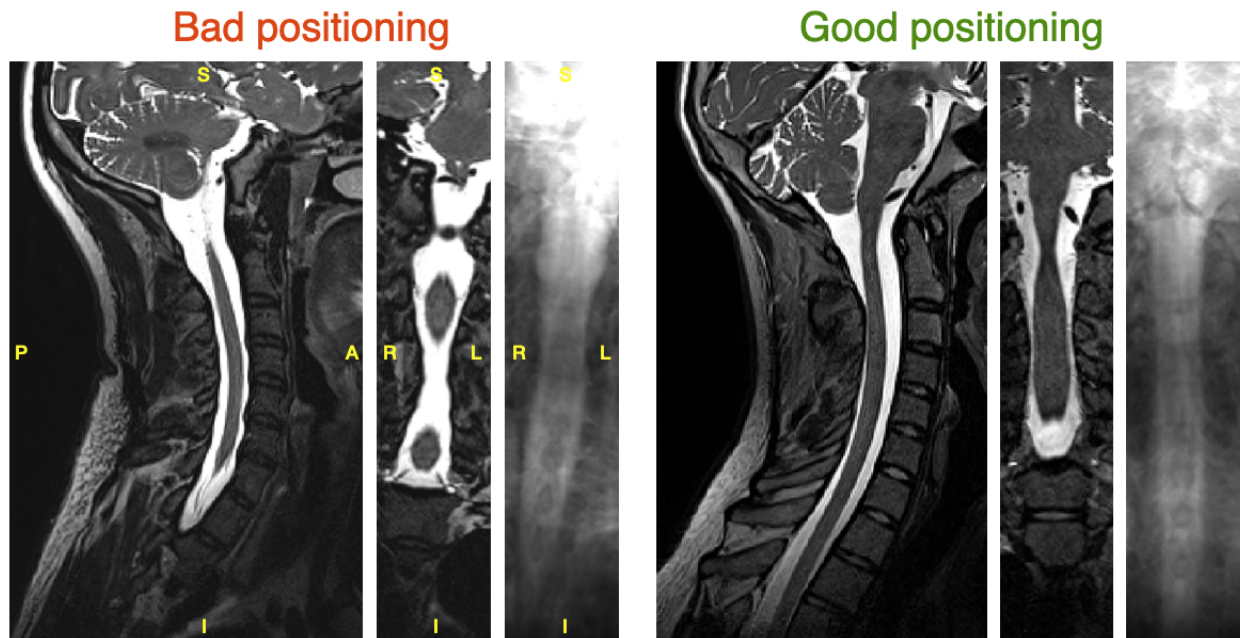
Bad positioning

Good positioning

Figure S4. T2w images illustrating a subject improperly aligned in the scanner (left). The effect could have been mitigated by rotating the FOV to align it with the medial plane (right). Left and right panels show views of the sagittal plane, coronal plane and a coronal plane with all slices averaged to highlight the orientation of the spine.
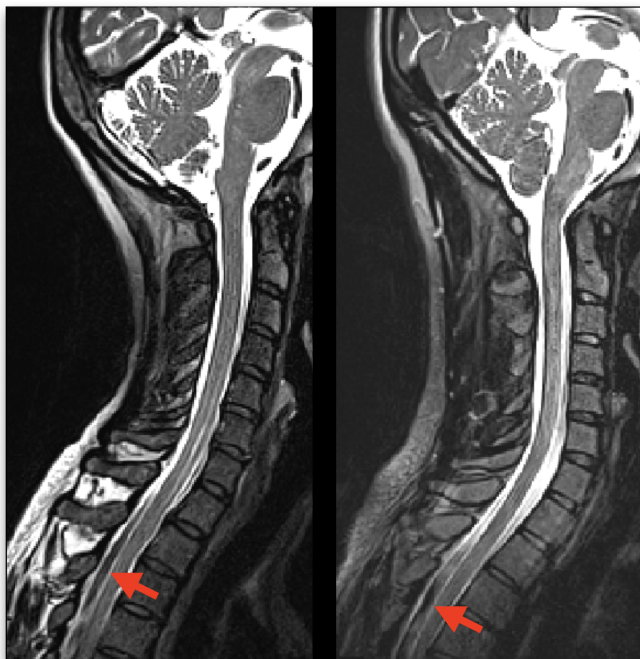

Figure S5. T2w scans showing signal drops in the CSF likely due to a poorly-recovered CSF signal combined with flow effects. These two subjects were acquired with FA = 180° instead of the recommended 120°, which likely explained the presence of those artifacts. A TR shorter than the recommended value would produce a similar artifact, due to insufficient T1 recovery in the CSF.
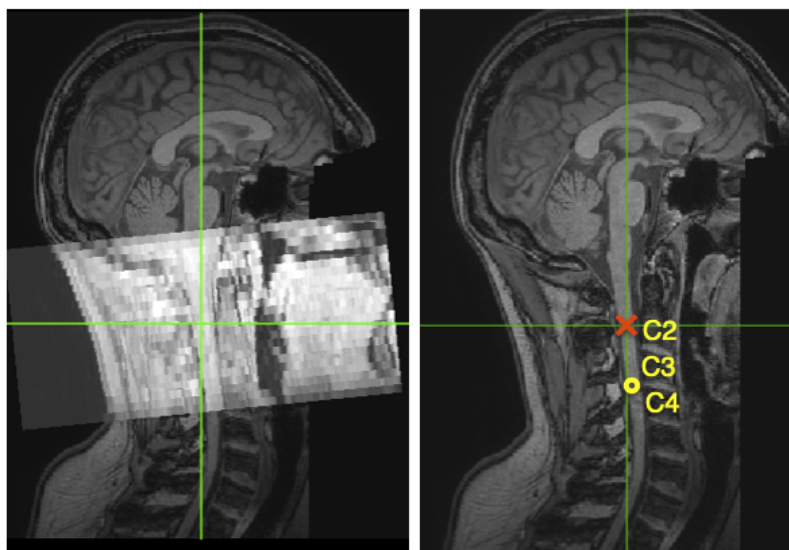
Figure S6. The left panel shows a GRE-MT image overlaid on a T1w image. The green cross is at the center of the FOV of the GRE-MT image. The right panel shows the T1w image without the overlay. There, we can see that the GRE-MT FOV is centered at the C2 vertebrae, whereas the requested FOV center was at the level of the C3-C4 intervertebral disc (step 9).
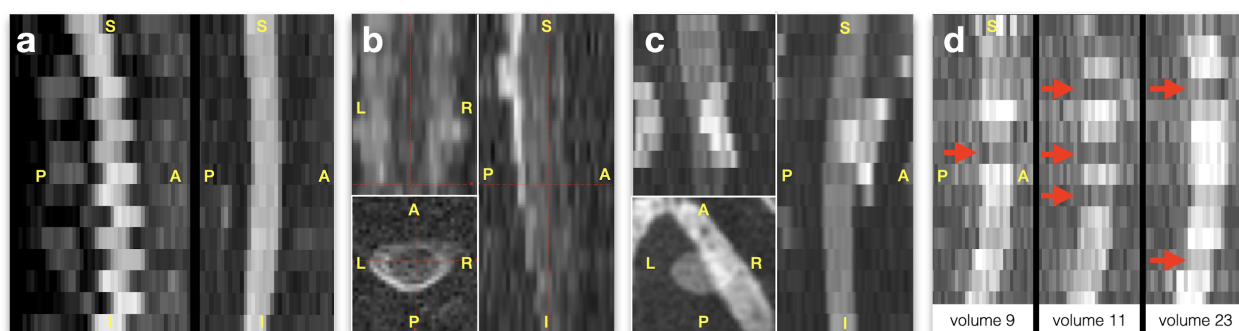

Figure S7. (a) Mean DWI scan from a Philips site (left) with a concatenated acquisition wherein odd slices are acquired during the first half of the entire acquisition (spanning all b-vectors) and the even slices are acquired during the second half. In the event of subject motion between those two acquisition sub-sets, apparent motion will be visible between the odd and even slices. When odd and even slices are acquired closer in time (in ascending/descending mode, or interleaved but sequentially within the same b-vector), this artifact is not visible (right). Such an artifact could be problematic for image registration with regularization along the S-I axis, or for performing diffusion tractography. (b) b=0 image from a DWI scan acquired with poor shimming and resulting signal dropout. (c) Another example of poor shimming resulting in sub-efficient fat saturation, with the fat being aliased on top of the SC. Here we show the mean DWI scan of a subject. (d) Effect of pulsatile effects on a non-cardiac gated acquisition. Diffusion-weighted scans (sagittal view) acquired at three b-vecs fairly orthogonal to the SC (i.e., diffusion-specific signal attenuation should be minimum in the SC), showing abrupt signal drop at a few slices (red arrows), likely due to cardiac-related pulsatile effects.

References

1. Topfer R, Starewicz P, Lo K-M, Metzemaekers K, Jette D, Hetherington HP, Stikov N, Cohen-Adad J. A 24-channel shim array for the human spinal cord: Design, evaluation, and application. Magn Reson Med. 2016 Nov;76(5):1604–11.

2. Topfer R, Foias A, Stikov N, Cohen-Adad J. Real-time correction of respiration-induced distortions in the human spinal cord using a 24-channel shim array. Magn Reson Med. 2018 Sep;80(3):935–46.

3. Islam H, Law CSW, Weber KA, Mackey SC, Glover GH. Dynamic per slice shimming for simultaneous brain and spinal cord fMRI [Internet]. Vol. 81, Magnetic Resonance in Medicine. 2019. p. 825–38. Available from: http://dx.doi.org/10.1002/mrm.27388

4. Finsterbusch J, Eippert F, Buchel C. Single, slice-specific z-shim gradient pulses improve T2*-weighted imaging of the spinal cord. Neuroimage. 2012;59:2307–15.

5. Finsterbusch J. B0 Inhomogeneity and Shimming. In: Quantitative MRI of the Spinal Cord, Elsevier, J Cohen-Adad and CAM Wheeler-Kingshott, eds. 2014;68–88.

6. Verma T, Cohen-Adad J. Effect of respiration on the B0 field in the human spinal cord at 3T. Magn Reson Med. 2014;72:1629–36.

7. Vannesjo SJ, Miller KL, Clare S, Tracey I. Spatiotemporal characterization of breathing-induced B0field fluctuations in the cervical spinal cord at 7T. Neuroimage. 2018 Feb 15;167:191–202.

8. van Gelderen P, de Zwart JA, Starewicz P, Hinks RS, Duyn JH. Real-time shimming to compensate for respiration-induced B0 fluctuations. Magn Reson Med. 2007;57:362–8.

9. Porter DA, Heidemann RM. High resolution diffusion-weighted imaging using readout-segmented echo-planar imaging, parallel imaging and a two-dimensional navigator-based reacquisition. Magn Reson Med. 2009;62:468–75.

10. Barry RL, Klassen LM, Williams JM, Menon RS. Hybrid two-dimensional navigator correction: a new technique to suppress respiratory-induced physiological noise in multi-shot echo-planar functional MRI. Neuroimage. 2008 Feb 1;39(3):1142–50.

11. Rasoanandrianina H, Massire A, Taso M, Guye M, Ranjeva J, Kober T, Callot V. Regional T 1 mapping of the whole cervical spinal cord using an optimized MP2RAGE sequence [Internet]. NMR in Biomedicine. 2019. Available from: http://dx.doi.org/10.1002/nbm.4142

12. Boudreau M, Tardif CL, Stikov N, Sled JG, Lee W, Pike GB. B1 mapping for bias-correction in quantitative T1 imaging of the brain at 3T using standard pulse sequences. J Magn Reson Imaging. 2017 Dec;46(6):1673–82.

13. Helms G. Correction for residual effects of B1+ inhomogeniety on MT saturation in FLASH-based multi-parameter mapping of the brain. In. Available from: https://cds.ismrm.org/protected/15MPresentations/abstracts/3360.pdf

14. Gilbert KM, Curtis AT, Gati JS, Klassen LM, Menon RS. A radiofrequency coil to facilitate B_1^+ shimming and parallel imaging acceleration in three dimensions at 7 T. NMR Biomed.

2011 Aug;24(7):815–23.

15. Chung S, Kim D, Breton E, Axel L. Rapid B1+ mapping using a preconditioning RF pulse with TurboFLASH readout. Magn Reson Med. 2010 Aug;64(2):439–46.

16. Lutti A, Hutton C, Finsterbusch J, Helms G, Weiskopf N. Optimization and validation of methods for mapping of the radiofrequency transmit field at 3T. Magn Reson Med. 2010 Jul;64(1):229–38.

17. Yarnykh VL. Actual flip-angle imaging in the pulsed steady state: a method for rapid three-dimensional mapping of the transmitted radiofrequency field. Magn Reson Med. 2007 Jan;57(1):192–200.

18. Nehrke K, Börnert P. DREAM—a novel approach for robust, ultrafast, multislice B1 mapping. Magn Reson Med. 2012;68(5):1517–26.

19. Sacolick LI, Wiesinger F, Hancu I, Vogel MW. B1 mapping by Bloch-Siegert shift. Magn Reson Med. 2010 May;63(5):1315–22.

20. Nelson F, Poonawalla AH, Hou P, Huang F, Wolinsky JS, Narayana PA. Improved identification of intracortical lesions in multiple sclerosis with phase-sensitive inversion recovery in combination with fast double inversion recovery MR imaging. AJNR Am J Neuroradiol. 2007;28(9):1645–9.

21. Poonawalla AH, Hou P, Nelson FA, Wolinsky JS, Narayana PA. Cervical spinal cord lesions in multiple sclerosis: T1-weighted inversion-recovery MR imaging with phase-sensitive reconstruction. Radiology. 2008;246(1):258–64.

22. Alcaide-Leon P, Cybulsky K, Sankar S, Casserly C, Leung G, Hohol M, Selchen D, Montalban X, Bharatha A, Oh J. Quantitative spinal cord MRI in radiologically isolated syndrome [Internet]. Vol. 5, Neurology - Neuroimmunology Neuroinflammation. 2018. p. e436. Available from: http://dx.doi.org/10.1212/nxi.0000000000000436

23. Kearney H, Miszkiel KA, Yiannakas MC, Ciccarelli O, Miller DH. A pilot MRI study of white and grey matter involvement by multiple sclerosis spinal cord lesions. Mult Scler Relat Disord. 2013 Apr;2(2):103–8.

24. Kearney H, Yiannakas MC, Abdel-Aziz K, Wheeler-Kingshott CAM, Altmann DR, Ciccarelli O, Miller DH. Improved MRI quantification of spinal cord atrophy in multiple sclerosis. J Magn Reson Imaging. 2014 Mar;39(3):617–23.

25. Papinutto N, Schlaeger R, Panara V, Caverzasi E, Ahn S, Johnson KJ, Zhu AH, Stern WA, Laub G, Hauser SL, Others. 2D phase-sensitive inversion recovery imaging to measure in vivo spinal cord gray and white matter areas in clinically feasible acquisition times. J Magn Reson Imaging. 2015;42(3):698–708.

26. Papinutto N, Henry RG. Evaluation of intra-and interscanner reliability of MRI protocols for spinal cord gray matter and total cross-sectional area measurements. J Magn Reson Imaging. 2019;49(4):1078–90.

27. Schlaeger R, Papinutto N, Panara V, Bevan C, Lobach IV, Bucci M, Caverzasi E, Gelfand JM, Green AJ, Jordan KM, Stern WA, von Büdingen H-C, Waubant E, Zhu AH, Goodin DS,

Cree BAC, Hauser SL, Henry RG. Spinal cord gray matter atrophy correlates with multiple sclerosis disability. Ann Neurol. 2014 Oct;76(4):568–80.

28. Bonacchi R, Pagani E, Meani A, Cacciaguerra L, Preziosa P, De Meo E, Filippi M, Rocca MA. Clinical Relevance of Multiparametric MRI Assessment of Cervical Cord Damage in Multiple Sclerosis [Internet]. Radiology. 2020. p. 200430. Available from: http://dx.doi.org/10.1148/radiol.2020200430

29. Olney NT, Bischof A, Rosen H, Caverzasi E, Stern WA, Lomen-Hoerth C, Miller BL, Henry RG, Papinutto N. Measurement of spinal cord atrophy using phase sensitive inversion recovery (PSIR) imaging in motor neuron disease. PLoS One. 2018 Nov 29;13(11):e0208255.

30. Papinutto N, Schlaeger R, Panara V, Zhu AH, Caverzasi E, Stern WA, Hauser SL, Henry RG. Age, Gender and Normalization Covariates for Spinal Cord Gray Matter and Total Cross-Sectional Areas at Cervical and Thoracic Levels: A 2D Phase Sensitive Inversion Recovery Imaging Study. PLoS One. 2015;10(3):e0118576.

31. Papinutto N, Asteggiano C, Bischof A, Gundel TJ, Caverzasi E, Stern WA, Bastianello S, Hauser SL, Henry RG. Intersubject Variability and Normalization Strategies for Spinal Cord Total Cross‑Sectional and Gray Matter Areas. J Neuroimaging. 2020 Jan 30;30(1):110–8.

32. Yiannakas MC, Kearney H, Samson RS, Chard DT, Ciccarelli O, Miller DH, Wheeler-Kingshott CAM. Feasibility of grey matter and white matter segmentation of the upper cervical cord in vivo: A pilot study with application to magnetisation transfer measurements. Neuroimage. 2012;63:1054–9.

33. Bellec P, Boyle JA. Bridging the gap between perception and action: the case for neuroimaging, AI and video games [Internet]. 2019. Available from: psyarxiv.com/3epws